Detection of Natural Abundance Nitrogen-15 through Phosphorus-31 Using Pulsed Field Gradients

Rodrigo J. Carbajo*[,1] and Fernando López-Ortiz†[,2]

*Departamento de Química Orgánica e Inorgánica, Universidad de Oviedo, Julián Clavería 8, 33006 Oviedo, Spain; and
†Área de Química Orgánica, Universidad de Almería, Carretera de Sacramento s/n, 04120 Almería, Spain

DEDICATED TO PROF. DR. H. GÜNTHER ON THE OCCASION OF HIS 65TH BIRTHDAY

NMR characterization of natural abundance ^{15}N in phosphorus–nitrogen compounds can be performed through ^{31}P using inverse detection methods. When the ^{31}P–^{15}N scalar coupling is small, its observation is greatly disturbed by the residual signal coming from the 99.6% abundant ^{14}N isotopomer that usually is not completely suppressed by the phase cycle of the sequence. The combined use of pulsed field gradients to suppress this residual signal and the enhanced sensitivity ^{31}P, ^{15}N{^{1}H}-esHSQC experiment affords artifact-free spectra with good signal-to-noise ratio, which allows the accurate measurement of ^{15}N NMR parameters such as chemical shifts and coupling constants with the benefits of phosphorus detection. © 2001 Academic Press

Key Words: ^{15}N; ^{31}P; PFG; HSQC; triple resonance.

INTRODUCTION

NMR data originating from the nitrogen-15 nucleus can provide good insight into a wide range of physical and chemical properties of organic, inorganic, and biomolecules: coordination mode, protonation, hydrogen bonding, configurational geometry, conformational relations, *cis–trans* or *syn–anti* stereochemistry, equilibrium systems, reaction mechanisms, biosynthesis, etc. (*1, 2*). However, the detection of ^{15}N in NMR is not always straightforward. The isotope nitrogen-15 has a very low natural abundance (0.37%), and a small and negative gyromagnetic constant, which results in a very low receptivity. Additionally the usually long T_1 values for ^{15}N increase the difficulties of its direct detection (*3*). In the case of biomolecular NMR, the nowadays-standard use of nitrogen-15-labeled samples has overcome the problem to observe ^{15}N. However, this method is not of general applicability. The preparation of ^{15}N-labeled organic and inorganic synthetic compounds normally requires the use of very expensive materials and troublesome procedures. For this kind of molecules polarization transfer and inverse detection schemes can partially solve the

problem, the latter methods usually giving better results. They select the nitrogen-15 nuclei scalarly coupled to a nucleus of high receptivity (mainly ^{1}H), eliminating throughout the experiment the signals coming from the abundant isotope ^{14}N (99.63%).

As mentioned above, the ^{1}H nucleus has been traditionally used for the indirect detection of ^{15}N in natural abundance, although the methodology can be extended to other highly receptive nuclei. These alternative nuclei have to be used when no protons are available in the molecule under study, or the ^{15}N–^{1}H coupling is very small or simply does not exist (*4*). Phosphorus-31 represents the best choice for a large number of organic and organometallic compounds. It is a 100% abundant $\frac{1}{2}$ spin nucleus and has been extensively employed in the indirect detection of metal nuclei (*5*). Also some biomolecular NMR experiments have taken advantage of the presence of phosphorus in nucleotides (*6*). In spite of its general availability, there are relatively few examples in the literature making use of the ^{31}P nucleus for the characterization of nitrogen-15 in nonbiological compounds. The first applications were based on phosphorus-to-nitrogen polarization transfer schemes INEPT (*7*) and DEPT (*8, 9*). For the ^{31}P and ^{31}N pair of nuclei indirect detection techniques may afford higher S/N ratios than polarization transfer methods by a factor $(\gamma_P/\gamma_N)^{3/2} = 13.3$. Recently, we have reported the first application of ^{15}N NMR data measurements using indirect detection through phosphorus (*10, 11*) based on the HMQC (*12*) pulse scheme. Throughout the experiment the protons are continuously decoupled to suppress the ^{31}P–^{1}H coupling, thereby increasing the signal-to-noise ratio.

The HMQC experiment showed a good sensitivity even for broad signals which is especially important in the natural abundance determination of ^{15}N in compounds where the phosphorus is bonded to two nitrogen atoms, as in polyphosphazenes, due to second-class relaxation coming from the quadrupolar ^{14}N nucleus coupled to ^{31}P (*13*). The combination of 1D and 2D experiments afforded ^{15}N chemical shifts and ^{31}P–^{15}N coupling constants as well as the measurement of isotopic

---

[1] Present address: MRC Laboratory of Molecular Biology, Hills Road, Cambridge CB2 2QH, UK.

[2] To whom correspondence should be addressed. E-mail: flortiz@ualm.es.

FIG. 1. Pulse scheme of the ^{31}P, $^{15}N\{^1H\}$ HSQC with enhanced sensitivity experiment. Narrow and wide bars correspond to flip angles of 90° and 180°, respectively. All pulses phases are x, unless specified. The pulse widths used were 9.6 and 23 μs for ^{31}P and ^{15}N, respectively, using an attenuation level of 1 dB for both heteronuclei. Composite pulse decoupling on the ^1H channel is used throughout the entire pulse sequence, with a ^1H pulse of 85 μs for an attenuation level of 23 dB. The delay Δ is set according to the size of the coupling to detect, following the relation $\Delta = 1/4J$. The time τ has the same duration as the pulsed field gradient (1 ms). In the 1D version of the experiment the time t_1 is made constant. Quadrature in the F_1 dimension is obtained by the *echo–antiecho* method, recording every transient twice and changing the sign of G_2 in the second scan. Gradients are sine-bell shaped, Z-axis directed, with durations of 1 ms each and peak amplitudes (G/cm) $G_1 = 40$, $G_2 = \pm 10$.

effects induced by the substitution of ^{14}N by ^{15}N. However, the reliability of the method dramatically diminishes when trying to observe very small $^{31}P–^{15}N$ couplings (1–5 Hz) as a consequence of the overlap of the multiplet with the residual signal coming from the ^{31}P coupled to ^{14}N, not perfectly suppressed by the phase cycling of the sequence. The most evident alternative to effectively suppress this residual signal and observe the small couplings is the use of pulsed field gradients (*14*).

In this paper we describe for the first time the application of an indirect detection method to observe natural abundance ^{15}N through ^{31}P incorporating pulsed field gradients. The enhanced sensitivity HSQC pulse sequence is adapted for this purpose, allowing accurate determination of ^{15}N chemical shift parameters and in particular small coupling constants, not easily accessible through the known preexistent methods.

RESULTS

The pulse sequence applied (Fig. 1) is the enhanced sensitivity HSQC (esHSQC) that includes pulsed field gradients and makes use of the *echo–antiecho* protocol by changing the sign of the last gradient (*15*). It has been converted into a triple-resonance experiment introducing the ^1H decoupling throughout the experiment to eliminate the $^{31}P–^1H$ couplings. As far as we know, this is the first time an HSQC experiment is used to detect ^{15}N through ^{31}P, with and without pulsed field gradients. The proportional amplitude of the gradients has to be calculated according to the gyromagnetic ratios of the two nuclei involved (in this case $\gamma_P = -3.996\gamma_N \sim -4\gamma_N$), resulting in a ratio $4:\pm1$ for the pulse sequence depicted in Fig. 1.

The benefits arising from the use of the pulsed field gradients in the esHSQC are readily seen when we compare the results of this experiment with those obtained with the phase-cycled pulse sequences HMQC and HSQC. A 1D ^{31}P, $^{15}N\{^1H\}$ spec-

trum was acquired with the three pulse sequences for a sample of *P*-(diphenyl)methyl(*N*-methoxycarbonyl)phosphazene, **1**, which shows a $^1J(^{31}P, ^{15}N)$ coupling of 37.0 Hz (Fig. 2). The ^{15}N satellites coming from the coupling with the phosphorus nucleus can be clearly seen in all three ^{31}P spectra. Traces (a) and (b) in Fig. 2 have been obtained with the phase-cycled pulse schemes HMQC and HSQC, respectively, while spec-

FIG. 2. Sections of the 161.98-MHz (400 MHz for ^1H, Bruker AMX400) 1D ^{31}P, $^{15}N\{^1H\}$ experiments showing the ^{31}P, ^{15}N doublet for a 0.6 M sample of *P*-(diphenyl)methyl(*N*-methoxycarbonyl)phosphazene, **1**, in CDCl₃. All experiments were recorded at 298 K with 256 scans, ^{31}P spectral width of 3000 Hz, preacquisition delay of 3 s, and coupling evolution time of 13.9 ms for a total duration of 31 min. Processed with an exponential weighting function (LB = 1). (a) HMQC sequence without pulsed field gradients, (b) HSQC without PFG, and (c) using the enhanced sensitivity HSQC pulse sequence depicted in Fig. 1, with gradient amplitudes 40:-10. Spectra (a) and (b) have been acquired without refocusing delay to minimize signal intensity losses. The relative intensities of the signals are 1:0.92:0.75.

trum (c) corresponds to the PFG esHSQC sequence. In terms of sensitivity, the HSQC-based pulse sequences show lower S/N ratio than the HMQC experiment (S/N for spectra a:b:c is 1:0.92:0.75). The small intensity differences observed between the spectra (a) and (b) may be assigned to the increased number of pulses of the HSQC vs the HMQC pulse scheme. For the experiment including pulsed field gradients a larger reduction in the S/N could be expected mainly because one of the coherence pathways giving rise to the signal is effectively suppressed by the gradients. Furthermore, the PFG esHSQC has the longest duration and increased number of pulses with respect to the other two experiments, factors that may result in a diminished S/N. The loss of only 25% in sensitivity compared with the HMQC experiment indicates a very good performance of the PFG esHSQC sequence. Even so, the main feature of the PFG esHSQC experiment is that it provides the expected perfect suppression of the residual signal coming from the $^{31}P–^{14}N$ isotopomers as can be observed in spectrum (c), Fig. 2, whereas the phase cycle of the nongradient HMQC (a) and HSQC (b) is unable to completely eliminate the above-mentioned signal.

In the example above the relative large size of the $^{31}P–^{15}N$ coupling does not interfere with the residual signal. α-Azidophosphazene, **2** (*16*), is a more challenging compound to prove the usefulness of the new method for the measurement of small $^{31}P–^{15}N$ coupling constants. This molecule presents four nitrogen atoms that may be, *a priori,* detected through the phosphorus provided that there is a resolved $^{31}P–^{15}N$ coupling. The 2D ^{31}P, $^{15}N\{^1H\}$ experiments acquired without and with gradients are given in Fig. 3. The nongradient HMQC TPPI experiment (a) shows two correlations between ^{31}P and ^{15}N, corresponding to nitrogen atoms N^1 ($\delta = -293.0$ ppm) and N^2 ($\delta = -302.9$ ppm), while a hypothetical cross peak arising from nitrogens N^3 and N^4 would be overlapped with the band of noise generated by the residual signal not suppressed by the phase cycle. Instead, in the PFG esHSQC a third cross peak can be observed and its chemical shift determined ($\delta(N^3) = -132.3$ ppm). A further advantage of the 2D PFG esHSQC experiment comes from the expected sensitivity increment compared with the phase-cycled one, reaching a 26% S/N increase in the case shown.

The inherent low resolution of the 2D experiments precludes an accurate measurement of the coupling constants between the ^{31}P and ^{15}N nuclei. Therefore it is necessary to record high-resolution 1D spectra as shown in Fig. 4. The different spectra have been acquired with and without gradients, and the evolution times in the sequence optimized for the various ranges of coupling constants to be measured. The first pair of experiments (a) and (d) was set to detect the largest coupling between the phosphorus atom and nitrogen N^1. While this coupling is clearly observed in both experiments ($^1J_{PN} = 39.9$ Hz), in the PFG-acquired spectrum (d) the coupling with nitrogen N^2 (indicated with *) can be guessed from the noise, whereas in the phase-cycled spectrum (a) the intense dispersion residual signal precludes its observation. Any-
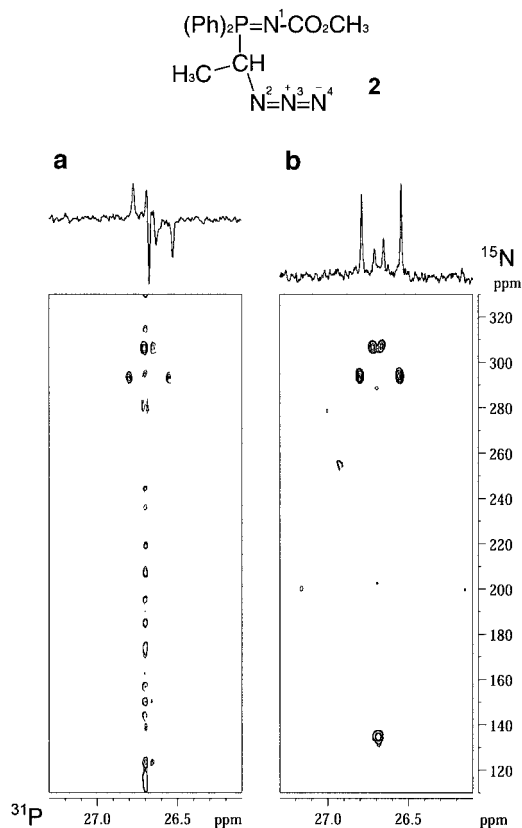

FIG. 3. Sections of the 2D ^{31}P, $^{15}N\{^1H\}$ spectra of **2** (0.25 M, CDCl$_3$). Both experiments were recorded at 298 K with 128 scans and 128 increments in t_1, spectral width of 1300 and 12,100 Hz in F_2 and F_1, respectively, preacquisition delay of 2 s, and coupling evolution time of 60 ms for a total duration of 10 h 20 min. (a) HMQC TPPI experiment without PFG showing just two correlations of the ^{31}P with nitrogens N^1 and N^2. Cross peaks are in antiphase because no refocusing delay was used to minimize magnetization losses. (b) Enhanced sensitivity HSQC pulse sequence of Fig. 1, which besides the correlations seen in spectrum (a) shows an additional cross peak with N^3. The 1D projections in the upper part of the 2D spectra have been acquired with the 1D version of the pulse sequences.

way, the coupling between the phosphorus and N^2 can be measured in both cases when the pulse sequences are optimized for this coupling (spectra (b) and (e), $^2J_{PN} = 9.1$ Hz). But the most remarkable improvement achieved with the PFG esHSQC experiment comes when trying to detect and measure very small $^{31}P–^{15}N$ couplings as that arising from nitrogen N^3. In the case of the phase-cycled experiment set to detect very small couplings (spectrum (c), Fig. 4, evolution time = 120 ms) the intense residual signal prevents the observation of any multiplet. In contrast, the PFG spectrum (f) shows a clean doublet coming from the three-bond coupling of the phosphorus with nitrogen N^3 ($^3J_{PN} = 4.0$ Hz).

CONCLUSIONS

We have described the first pulsed field gradient experiment based on the PFG esHSQC sequence for the detection of
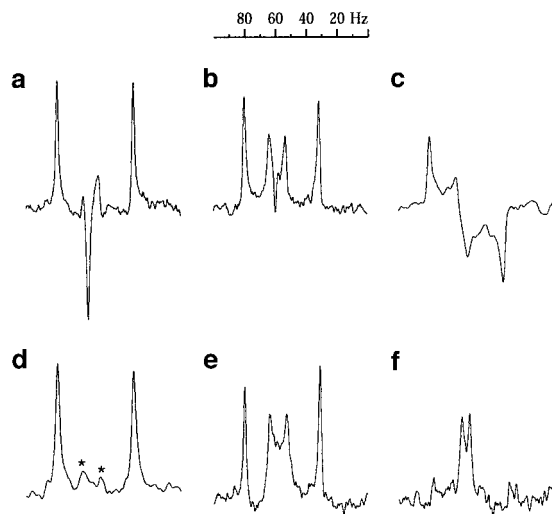
FIG. 4.   1D ^{31}P, ^{15}N{1H} spectra of **2**, recorded at 298 K to observe the couplings between ^{31}P and the different nitrogen atoms in the molecule. Every experiment was recorded with 1024 scans, 2 s of preacquisition delay, for a total duration of 3 h and a final resolution of 0.03 Hz/pt. Spectra (a)–(c) were recorded with the HMQC sequence without PFG, and (d)–(f) were recorded using the enhanced sensitivity HSQC experiment depicted in Fig. 1. Spectrum (c) was acquired without refocusing in order to distinguish the smallest ^{31}P, ^{15}N coupling from the residual ^{31}P, ^{14}N signal. The evolution time for every pair of experiments is (a), (d) = 13.4 ms; (b), (e) = 34 ms; and (c), (f) = 120 ms.

natural abundance ^{15}N NMR parameters through ^{31}P. Artifact-free 2D spectra are obtained with enhanced sensitivity compared to the phase-cycled HMQC scheme. The resulting high-quality spectra allow the observation of ^{31}P, ^{15}N correlations arising from very small couplings, which would be otherwise obscured by the residual signal of the ^{31}P, ^{14}N isotopomers. The precise values of these coupling constants can be measured by carrying out the experiment in the 1D mode. The importance of this type of experiments will show up mainly in the detection of natural abundance ^{15}N for organic (*17*) and inorganic molecules (*18*) where no ^{1}H atom is available to be used as the source of magnetization.

ACKNOWLEDGMENTS

REFERENCES

1. J. Mason, Nitrogen, *in* "Multinuclear NMR" (J. Mason, Ed.), pp 335–368, Plenum Press, New York (1987).

2. M. Witanowski, L. Stefaniak, and G. A. Webb, Nitrogen NMR Spectroscopy, *Annu. Rep. NMR Spectrosc.* **18**, 1–737 (1986).

3. G. C. Levy and R. L. Lichter, "Nitrogen-15 Nuclear Magnetic Resonance Spectroscopy," Wiley, New York (1979).

4. There is one report of the application of polarization transfer from ^{19}F to ^{15}N via INEPT to the study of some perfluorocompounds: A. Costa, M. Tato, and R. S. Matthews, N-15 INEPT spectra of some perfluoroazines, *Magn. Reson. Chem.* **6**, 547–548 (1986).

5. F. López-Ortiz and R. J. Carbajo, Applications of polarization transfer and indirect detection NMR spectroscopic methods based on phosphorus-31 in organic and organometallic chemistry, *Curr. Org. Chem.* **2**, 97–130 (1998).

6. G. Varani, F. Aboul-ela, and F. H. T. Allain, NMR investigation of RNA structure, *Prog. NMR Spectrosc.* **29**, 51–127 (1996).

7. S. J. Berners-Price, M. J. Dimartino, D. T. Hill, R. Kuroda, M. A. Mazid and P. J. Sadler, Tertiary phosphine complexes of gold(I) and gold(III) with imido ligands—^{1}H, ^{31}P and ^{15}N NMR-spectroscopy, antiinflammatory activity, and X-ray crystal-structure of (phthalimido) (triethylphosphine)gold(I), *Inorg. Chem.* **24**, 3425–3434 (1985).

8. D. Gudat, Polarization transfer between heteronuclei—application of ^{31}P, ^{15}N-polarization transfer techniques in ^{15}N-NMR spectroscopy of phosphorus–nitrogen compounds, *Magn. Reson. Chem.* **24**, 925–930 (1993).

9. D. Gudat, Applications of heteronuclear *X*, *Y*-correlation spectroscopy in organometallic and organoelement chemistry, *Annu. Rep. NMR. Spectrosc.* **38**, 139–202 (1999).

10. F. López-Ortiz, E. Peláez-Arango, and P. Gómez-Elipe, Nitrogen-15 NMR spectroscopy of phosphazenes based on phosphorus-31 detection, *J. Magn. Reson. A* **119**, 247–251 (1996), doi: 10.1006/jmra.1996.0080.

11. E. Peláez-Arango, F. J. García-Alonso, G. Carriedo, and F. López-Ortiz, ^{15}N NMR spectroscopy of cyclotriphosphazenes and polyphosphazenes based on ^{31}P, ^{15}N HMQC correlations, *J. Magn. Reson. A* **121**, 154–159 (1996), doi:10.1006/jmra.1996.0155.

12. A. Bax, R. H. Griffey, and B. L. Hawkins, Correlation of proton and ^{15}N chemical shifts by multiple quantum NMR, *J. Magn. Reson.* **55**, 301–315 (1983).

13. A. Abragam, "The Principles of Nuclear Magnetism," Oxford Univ. Press, London (1983).

14. J. Keeler, R. T. Clowes, A. Davis, and E. D. Laue, Pulsed-field gradients—Theory and practice, *Methods Enzymol.* **239**, 145–207 (1994).

15. L. E. Kay, P. Keifer, and T. Saarinen, Pure absorption gradient enhanced heteronuclear single quantum correlation spectroscopy with improved sensitivity, *J. Am. Chem. Soc.* **114**, 10663–10665 (1992).

16. J. Álvarez-Gutiérrez, C. Andújar-Sánchez, I. Pérez-Álvarez, and F. López-Ortiz, Electrophilic ammination of phosphazenes, manuscript in preparation.

17. F. López-Ortiz, E. Peláez-Arango, B. Tejerina, E. Pérez-Carreño, and S. García-Granda, Solution-state, solid-state, and calculated structures of an alpha-lithiated monophosphazene, *J. Am. Chem. Soc.* **117**, 9972–9981 (1995).

18. G. A. Carriedo, F. J. García-Alonso, J. L. García, R. J. Carbajo, and F. López-Ortiz, Synthesis and ^{1}H-, ^{15}N-, ^{31}P-, ^{183}W-multinuclear magnetic resonance study of the cyclotriphosphazenes [N3P3(dobp)2(OC5H4N-4)(2)] and [N3P3(dobp)(OC5H4N-4)(4)] and their W(CO)(5) complexes (dobp=2,2′-dioxybiphenyl), *Eur. J. Inorg. Chem.* 1015–1020 (1999).